PR7 Development on Neutron Imaging Application

Y. Saito

Research Reactor Institute, Kyoto University

1. Objectives and Allotted Research Subjects

Neutron imaging provides valuable information which cannot be obtained from an optical or X-ray imaging. The purpose of this project is to develop the imaging method itself and also the experimental environment for expanding the application area of the neutron imaging. The allotted research subjects are as follows:

ARS-1 Measurements of Multiphase Dynamics by Neutron Radiography (Y. Saito *et al.*)
ARS-2 Visualization and Measurement of Flow Behavior in Industrial Equipment (H. Asano *et al.*)
ARS-3 Visualization and Measurement of Adsorption/Desorption Process of Ethanol in Activated Carbon Adsorber for Adsorption Heat Pump (N. Asano *et al.*)
ARS-4 Visualization of heavy oil in packed bed reactor by neutron radiography (T. Tsukada *et al.*)
ARS-5 Characteristics of the Void Fraction under Transient Condition (H. Umekawa *et al.*)
ARS-6 Estimation of the Frosting and Defrosting Phenomena by Using Neutron Radiography (R. Matsumoto *et al.*)
ARS-7 Neutron imaging and optics development using simulation of VCAD Systems (Y. Yamagata *et al.*)
ARS-8 Water and Salt Distribution in a Rice Hull Medium under Sodium Chloride Solution Culture (U. Matsushima *et al.*)
ARS-9 Measurement of Water Content in Hardened Cement Paste by Neutron Imaging (T. Numao *et al.*)
ARS-10 In-situ Neutron Radiography Investigation on the Hydraulic Behavior of High Strength Cement Paste under High Temperature (M. Kanematsu *et al.*)
ARS-11 Evaluation of coolant distribution in a flat heat-pipe type heat spreader (K. Mizuta *et al.*)
ARS-12 Visualization of Organic Materials for Development of Industrial Applications (A. Uritani *et al.*)
ARS-13 Visualization of Coolant Flow in a Micro-Structured Wick (Y. Tsuji *et al.*)

2. Main results and the contents of this report

Due to the limitation of beam time at the KUR, all of the scheduled experiments could not be performed for fiscal 2017. However, some new results have been obtained and also the new imaging system was developed by X-ray imaging as follows:

ARS-1 applied X-ray and neutron imaging to two-phase flow behavior. Simultaneous measurement system with high frame-rate neutron and X-ray imaging was developed and the system was tested for the air-water two-phase flow.

ARS-2 and 3 applied neutron imaging to boiling two-phase flow in parallel mini-channel heat exchanger. HFC-134a and FC3283 were used as the refrigerant and the heat medium, respectively. The heat exchanger was manufactured by diffusion bonding of thin stainless steel plates, and consists of single-layer refrigerant and heating medium parallel channels. The neutron imaging system at the B4 port was utilized for the measurements, and that at E2 port was also utilized for preliminary experiments. From the experimental results, the effect of the inlet orifices have been investigated.

ARS-4 applied neutron imaging to the flow visualization of heavy oil in packed bed reactor. Heavy oil and N2 gas were supplied to the experimental apparatus, and they flowed co-currently through the packed bed, which consists of Al_2O_3 particles having the diameter of 1 or 3mm. From the experimental results, a flow channeling was observed depending on the experimental conditions.

ARS-5 applied the neutron imaging to microchannel heat exchanger and subcooled boiling. Quenching phenomena in the microchannel heat exchanger was visualized and the effect of flow direction was investigated for the subcooled boiling.

ARS-6 applied neutron imaging to frosting behavior in cooling heat exchange system. 3-D frost density was clearly visualized by the neutron CT imaging system at the B4 port.

ARS-12 performed quantification of neutron imaging by using two-different neutron source (KUR-E2 and NUANS). A detector indicated manufactured by J-PARC was used for the imaging and the spatial resolution of neutron imaging at the two neutron imaging facilities was compared each other.

ARS-13 developed new measurement technique of the superfluid. Helium excimer was used as the tracer in the superfluid helium. In the experiments at the B4 port, the emission of by helium excimer clusters via neutron-3He absorption reaction was clearly observed.

ARS-14 developed capillary-plate-based fluorescent plates and the detail characteristics were examined at the E2 port.

PR7-1 Dynamic Observation of Two-Phase Flow using Neutron Radiography

Y. Saito and D. Ito

Institute for Integrated Radiation and Nuclear Science, Kyoto University

INTRODUCTION: Neutron radiography (NRG) is a powerful tool for fluid flow visualization as well as two-phase flow research. Gas-liquid two-phase flows in a metallic pipe have been visualized clearly by using NRG. However, it would be still difficult to obtain dynamic information on such flows by NRG, because of insufficient neutron flux from neutron sources and poor efficiency of imaging devices. In this work, our imaging system was improved for high frame rate NRG. Then, the system was applied to air-water two-phase flow measurements in a circular pipe. In addition, a simultaneous measurement with X-ray radiography (XRG) was performed to compare the acquired transmission images of the two-phase flow.

EXPERIMENTS: Experiments were performed at the B-4 supermirror neutron guide facility [1] of the Institute of Integrated Radiation and Nuclear Science, Kyoto University. The neutron flux of the B-4 port is 7.5×10^7 n/cm^{2}s and the beam width and height at the beam exit are 10 mm and 75 mm, respectively. An imaging system for high frame rate NRG consists of a neutron converter, a dark box with a single mirror, an ultrasensitive lens, an optical image intensifier and a high-speed camera, as shown in Fig.1. In the present system, high sensitivity high-speed camera (AX-50, Photron) was applied to enhance the temporal resolution. In addition, XRG system was installed in the B-4 facility to compare the imaging results. The XRG system consists of an X-ray generator, an X-ray image intensifier and a high-speed camera. The applied voltage and current of the X-ray generator were 150 kV and 2.3 mA, respectively. These systems were arranged as the X-ray beam direction is perpendicular to the direction of the neutron beam, as shown in Fig.1. Two high-speed cameras and the optical image intensifier were synchronized for simultaneous observation.
The test section is a vertical circular pipe which is made from polycarbonate. The inner diameter is 20 mm and the wall thickness of the test pipe is 1 mm. The water was circulated by a pump and the compressed air was injected from the upstream of the test section. The flow rates of water and air were monitored by flow meters.

RESULTS: The typical neutron and X-ray transmission images of air bubble in water are shown in Fig.2. In the present experiments, the frame rate of 10,000 Hz could be achieved by using the improved NRG system. By comparing two images, they represent different characteristics. In the air-water two-phase flow, water has high neutron attenuation coefficient, therefore it is difficult to detect the small bubble in water. However, visualization of detailed flow structure will be possible by combining with X-ray imaging results. This simultaneous imaging technique would be useful for the clarification of multiphase flow dynamics such as steam explosion.

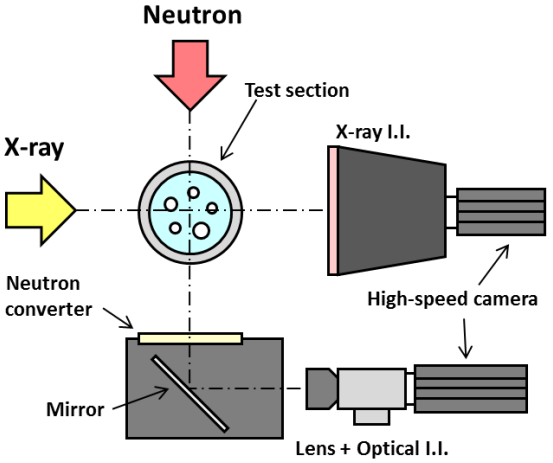

Fig. 1 Schematic diagram of simultaneous measurement with high frame-rate neutron and X-ray radiography systems.

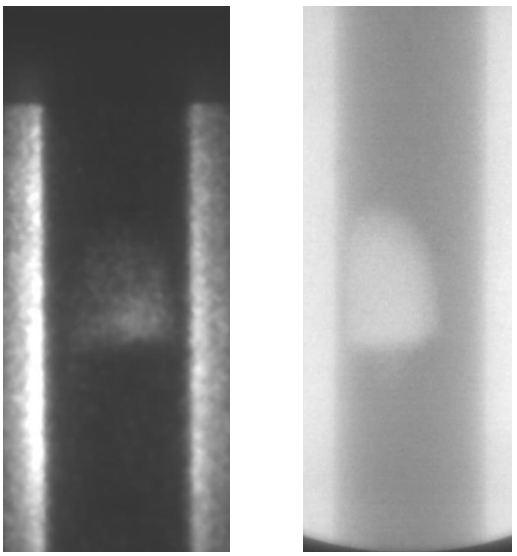

(a) NRG (10,000fps) (b) XRG (200 fps)

Fig. 2 Neutron and X-ray transmission images of air-water two-phase flow.

REFERENCE:

[1] Y. Saito, *et al*., Nucl. Instr. Meth. Phys. Res., A, **651** (2011) 36-41.

PR7-2

Visualization and Measurement of Boiling Flow Behaviors in Parallel Mini-channel Heat Exchanger

H. Asano, H. Murakawa, K. Sugimoto, R. Moriyasu, D. Ito[1] and Y. Saito[1]

Department of Mechanical Engineering, Kobe University
[1]Research Reactor Institute, Kyoto University

INTRODUCTION: Compactness and reduction in temperature difference between fluids are still strongly required for heat exchanger used in binary power cycles for waste heat utilization and refrigeration/heat pump systems. One of the way is to increase heat transfer area density. Microchannel compact heat exchanger manufactured by diffusion bonding process is developed. Since smaller diameter leads to larger pressure loss, micro channel heat exchanger has many parallel channels. Therefore, in the case that the heat exchanger is used for evaporator, refrigerant flow distribution often causes a deterioration in the heat transfer performance. On the aspect of heat exchanger, the temperature of heating medium will decrease by heat exchange in an evaporator. The temperature change means the decrease in temperature difference between fluids, and lead to the change in heat flux. It is important to understand the boiling flow distribution in parallel refrigerant channel. In this study, boiling flow behaviors in a single layer microchannel heat exchanger had been visualized by neutron radiography.

EXPERIMENTS: HFC-134a and FC3283 were used as the refrigerant and the heating medium, respectively. The configuration of the tested mini-channel heat exchanger is shown in Figure 1. The heat exchanger was manufactured by diffusion bonding of thin stainless steel plates, and consists of single-layer refrigerant and heating medium parallel channels. The number of channels are 21 for the refrigerant and 20 for the heating medium. Each channel has semicircular cross-section as shown in Fig. 1(b). The refrigerant channels were placed in crossed arrangement with the channels of the heating medium. The refrigerant was supplied to the vertically placed test section as a liquid single-phase flow close to saturated liquid, and evaporated by heating from FC3283. Since the temperature of FC3283 decreases in the flow direction, heat transfer rate will be higher on the left side due to the larger temperature difference. The neutron radiography system at B4 beam line was utilized for the measurements, and the system at E2 beam line was also utilized in the preliminary experiments. Radiographs on a scintillation converter were recorded by a cooled CCD camera with the exposure time of 30 seconds and the pixel size of 87.9 μm/pixel. Since the visualized area cannot cover the width of the test section, radiographs were taken by dividing 5 areas. Mass flux of the refrigerant and heating medium was set to 50, 100 kg/(m^2・s) and 460, 920 kg/(m^2・s), respectively.

RESULTS: Void fraction distributions can be obtained from some image processing using images with and without refrigerant. The obtained results of void fraction, α, distribution are shown in Fig. 2. At first, one dimensional distribution was measured for each channel. Then, the results for 21 channels are shown as an image with 21 pixels in horizontal. Void fractions are shown in color scale. Heat transfer rates are shown in Table 1 with the flow conditions. Fig. 2(b) shows the results for the test section with orifices at the inlet of each refrigerant channel for flow stabilization into parallel channels. Void fraction in the center region became higher. The reason might be maldistribution of refrigerant where mass flow rate was larger at the center. Void fraction through the right path was higher than the left path. The effect of the inlet orifices to improve the flow distribution was not observed in the experiments.

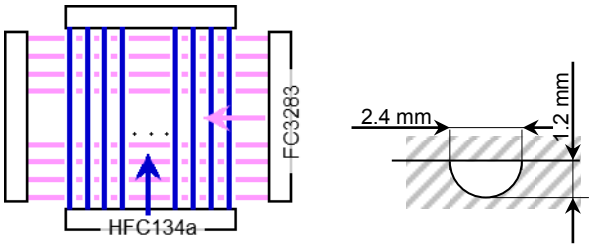

(a) Channel arrangement (b) Cross-section

Fig. 1 Channel configuration of cross-flow type evaporator.

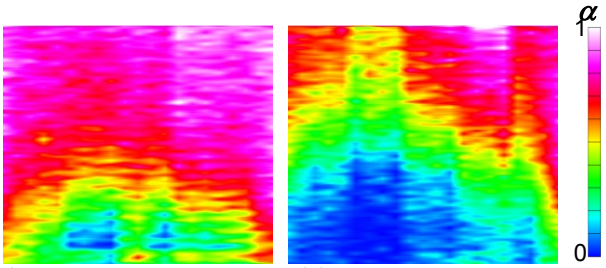

(a) Without inlet orifices (b) With inlet orifices

Fig. 2 Void fraction distribution.
(G_r=100 kg/(m^2・s), G_{FC}=460 kg/(m^2・s), T_{FCin}=47.2～47.3 ℃)

Table 1 Heat transfer performance.

	Fig. 3 (a)	Fig. 3 (b)
Refrigerant (HFC134a)		
Evaporating pressure [MPa]	0.585	0.632
Inlet temperature [℃]	19.5	19.8
Inlet subcooling degree [K]	1.3	3.5
Heating medium (FC3283)		
Inlet temperature [℃]	47.2	47.3
Outlet temperature [℃]	41.8	42.8
Heat transfer rate [W]	115.8	98.1

PR7-3 Flow Visualization of Heavy Oil in Packed Bed Reactor by Neutron Radiography

T. Tsukada, M. Kubo, E. Shoji, K. Yamagiwa, S. Takami[1], K. Sugimoto[2], D. Ito[3] and Y. Saito[3]

Dept. of Chemical Engineering, Tohoku University

[1] Dept. of Materials Science and Engineering, Nagoya University

[2] Dept. of Mechanical Engineering, Kobe University

[3] Institute for Integrated Radiation and Nuclear Science, Kyoto University

INTRODUCTION: With an increase in the demand for petrochemical feedstock and middle distillate, utilization of heavy oil such as atmospheric or vacuum residue is also necessary. Since the heavy oil has high viscosity and its quality is low, however, desulfurization and upgrading processes are required to use the heavy oil effectively. A trickle bed reactor, in which heavy oil and hydrogen gas are flowed concurrently through a packed bed of catalytic particles, is generally used in the upgrading process. Since channeling and consequent hot spots decrease the performance in the reactor, the understanding of flow behavior in the reactor is significant.

Recently, the development of CFD simulator of hydrodynamics and reactions in the reactor has been advanced to clarify the flow behavior. On the other hand, the experimental works on flow visualization of the heavy oil have not been conducted. This is because the reactor was made of metal for operation at high pressure and high temperature, and consequently the visualization using visible light was not available. Therefore, in this work, the flow visualization of heavy oil in the packed bed reactor was performed by neutron radiography.

EXPERIMENTS: In the neutron radiography for the flow visualization of heavy oil, the Kyoto university research reactor (KUR) was utilized as neutron source. Fig. 1 shows the schematic diagram of the apparatus used here. The heavy oil and N_2 gas were supplied concurrently to a packed bed reactor, i.e., a 1/2-inch stainless steel tube filled with Al_2O_3 particles having the diameter of 1 or 3 mm. Atmospheric residue (AR) was used as the heavy oil sample. The reactor was heated to temperatures of 100°C and 250°C to change the viscosity of heavy oil. The flow rate of heavy oil was set to 2.5 mL/min, while that of N_2 gas was changed. The reactor was operated at atmospheric pressure. An image intensifier and a CCD camera at the framerate of 30 fps were used to obtain visualization images of the unsteady flow behavior. An image processing to reduce noises was performed for the obtained images.

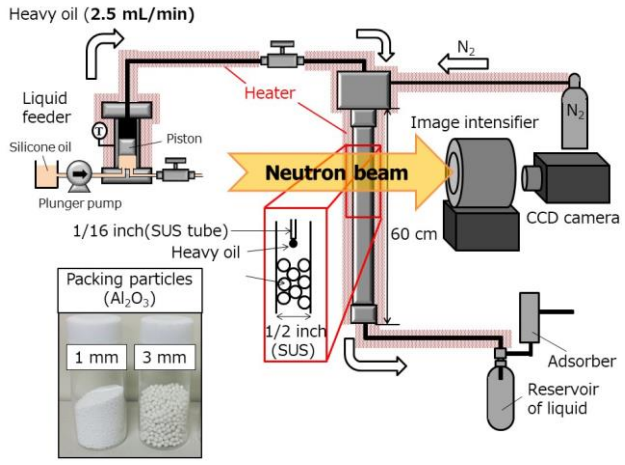

Fig. 1 Schematic diagram of experimental apparatus

RESULTS: The flow behavior of heavy oil in the reactor varied depending on the experimental conditions. Fig. 2 shows the effect of the temperature on the flow behavior of heavy oil in the reactor. Since the viscosity of heavy oil markedly varies with temperature, that is, the viscosity of heavy oil at 100°C is 10 times larger than that at 250°C, the head velocity of heavy oil flowing down at 100°C became approximately half that at 250°C for the particle diameter of 1 mm. In addition, the heavy oil at 100°C spread radially to the wall of the tube, whereas the heavy oil at 250°C did not spread. In the case of 3 mm particle diameter, the heavy oil did not spread at both 100°C and 250°C compared with the case of 1 mm particles, and the flow channeling occurred in the packed bed.

CONCLUSION: Neutron radiography is a useful technique to visualize the flow behavior of heavy oil in a packed bed reactor, whose wall was made of metal, at high temperature.

ACKNOWLEDGEMENT: This research was supported by Ministry of Economy, Trade and Industry (METI) and Japan Petroleum Energy Center (JPEC).

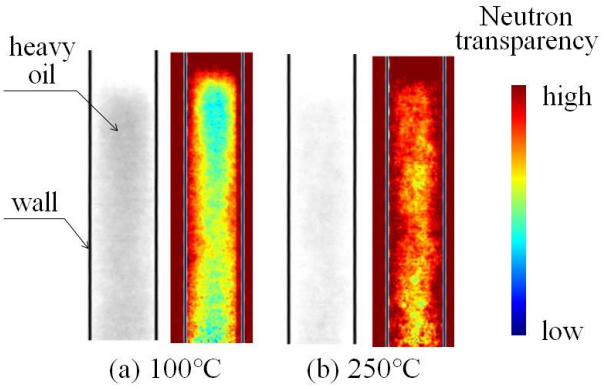

Fig. 2 Effect of reactor temperature on flow behavior in the reactor when the packing particle diameter is 1 mm and the flow rate of N_2 gas is 1 L/min. Here, the left side in (a) or (b) is the image after background subtraction, and the right side is the image converted by color mapping.

Trial Measurement of Void Fraction in Boiling Channel

H. Umekawa, T. Ami, M. Kitagawa, T. Kitanaka,
Y. Kawazoe, K. Saito, Y. Saito[1] and D. Ito[1]
Dept. Mechanical Engineering, Kansai University
[1]*Institute for Integrated Radiation and Nuclear Science, Kyoto University*

INTRODUCTION: Void fraction is a fundamental and important information of two-phase flow. As the measuring procedure of void fraction, neutron radiography has suitable performance, but several limitation exists. In this term, three trials have been done to evaluate the adaptability of neutron radiography to new object. In this report, these results are briefly introduced.

EXPERIMENTS:

1.Microchannel heat exchanger:

Recently microchannel heat-exchanger has been used by actual equipment, such as air conditioning unit. In these systems, the mal-distribution of the flow has not been fully understood under non-uniform heating condition. These heat exchanger has small parallel tubes with less than 1mm tube diameter, and gap between each channel is less than 0.1mm. Figure 1 is the example of the visualization results and photograph of microchannel heat exchanger. In this trial, working fluid, exposure period, beam slit to enhance the spatial resolution and construction of heat exchanger have been estimated.

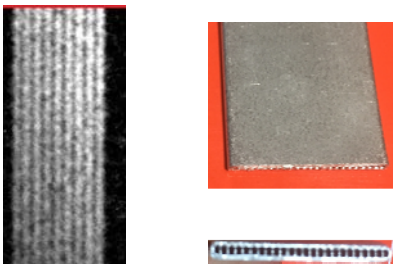

Fig. 1 Micro Channel Heat-exchanger.

2.Quenching Phenomena

During the quenching process of high temperature tubes, Inverted annular flow(IAF) will be generated. In this region, estimation of the void fraction is quite important, but enough data has not existed. To estimate the IAF, the quantitative measurement in dynamic process is required. In this trial, to decide the detail experimental condition and suitable frame rate to keep the spatial resolution, dynamic image was taken under several conditions. Figure 2 is example of successive image by using Neutron Image Intensifier and a high speed camera. As shown in these results, the liquid core movement is relatively slow owing to the large slip between liquid and vapor. It means the possibility of the measurement of void fraction of IAF by this procedure, but more enhancement of the spatial resolution is required.

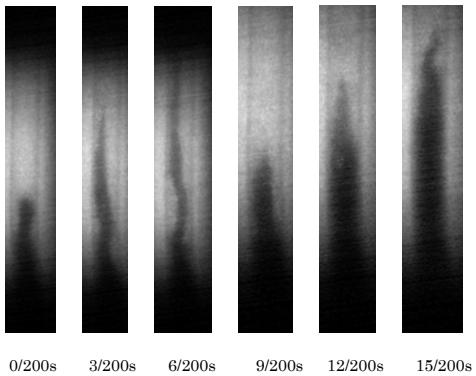

Fig.2 Quenching phenomena

3.Subcooled Boiling

In this investigation, void fraction under upward and downward flow condition were measured. Figure 3(a) is the void fraction distribution, and void fraction at 390mm obtained by changing the heat flus is plotted against thermal equilibrium quality in Fig.3(b). In this condition, upward flow and downward flow take a quite different tendency. Figure 3(c)is the same data with Fig.3(b), but solid line corresponds to the void fraction under same heat flux of different location. As shown in Figure, down ward flow condition takes quite different tendency influenced by magnitude of heat flux. This tendency may be explained by the effect of buoyancy.

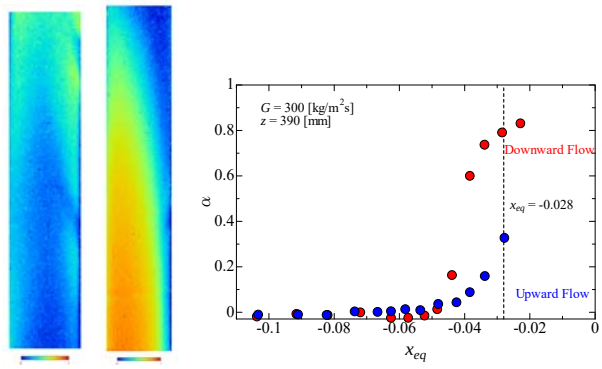

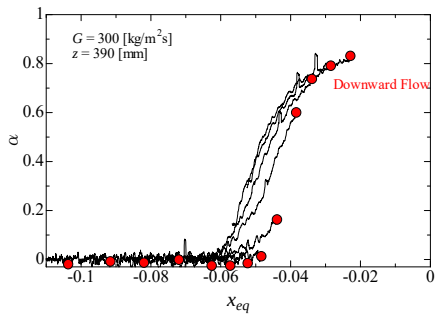

(c)

Fig.3 Void fraction of subcooled boiling

PR7-5 **Estimation of the Frost Formation on the Heat Exchanger by Using Neutron Radiography**

R. Matsumoto, T. Uechi[1], Y. Nagasawa[1], T. Shiokawa[1], D. Ito[2] and Y. Saito[2]

Faculty of Engineering Science, Kansai University
[1]Graduate School of Science and Engineering, Kansai University
[2]Institute for Integrated Radiation and Nuclear Science, Kyoto University

INTRODUCTION: Heat exchangers which are operated at 0 ºC below are subjected to occurring the frost deposition and its growth. The structure of frost is porous consisted of ice crystal and air. Therefore the thermal conductively is low, and the frost layer becomes the thermal resistance between the cooling surface and ambient air. Matsumoto et al. [1] reported the two dimensional distribution of the frost deposition rate on the plate fin-tube heat exchanger by using neutron radiography (NRG). Neutrons are strongly attenuated by the water molecules in the frost layer, but not by the aluminum heat exchanger. The frost formation can be quantitatively estimated based on the neutron beam attenuation. By applying the computed tomography, the three dimensional frost formation can be visualized. In this study, the three dimensional distribution of the frost deposition and the frost density profiles on the plate fin-tube heat exchanger are quantitatively estimated by using the neutron computed tomography imaging at KUR B-4 radiation port.

EXPERIMENTS: Fig.1 shows the schematic view of the experimental apparatus. Cooled humid air adjusted to the flow rate 70 L/min was supplied to the test section. The test section consisted of Styrofoam block duct with a cross section of 68 mm x 150 mm and the aluminum plate fin-tube heat exchanger. The heat exchanger consisted by 6 fins with 60 mm in height, 28 mm in width, 0.25 mm in thickness, and together with two tubes of an outer 8.5 mm. Fin pitch was 5 mm. The heat exchanger was cooled by -22 ºC fluorinert. The frosting duration was 60 min. CCD camera (Princeton Inst., 16-bit, 1024 ×1024 pixels) set in the inside a light-tight camera box. Two mirrors reflect the visible ray image from the converter with the 6LiFZnS scintillator screen mounted onto the front end of the camera box. 600 neutron radiography (NRG) images were taken by the CCD camera with an exposure time of 5 sec by rotating the heat exchanger through 180 degrees.

RESULTS: Fig.2(a) shows the digital camera image of the heat exchanger taken from the downstream-side. Frost covered the fins. Fig.2 (b) shows the NRG images after 60 min frosting duration. Frost formation on the plate fin and tube surfaces could be clearly visualized by neutron radiography. The tomographic image of x-y plate at a z position was reconstructed from the lateral linedate of 600 projection images. The tomographic image was expressed by the linear attenuation coefficient μ. The frost density ρ can be calculated from $\rho = \mu / \mu_{m,ice}$, in which $\mu_{m,ice}$ is the mass attenuation coefficient of ice. Fig.3 shows the three dimensional frost density distributions At the fin edge, high frost deposition are observed, however, the frost layer is thin in the wide area of the wake region. The three dimensional frost density profile can be estimated by using 3D neutron computed tomography.

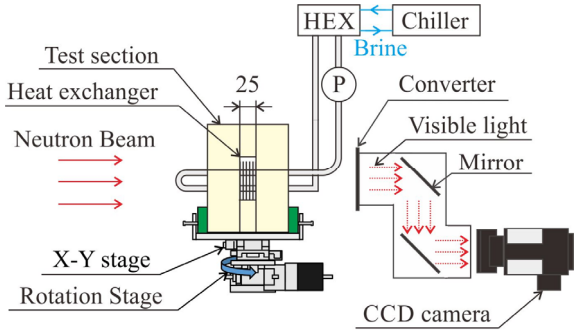

Fig.1 Schematic view of the experimental apparatus

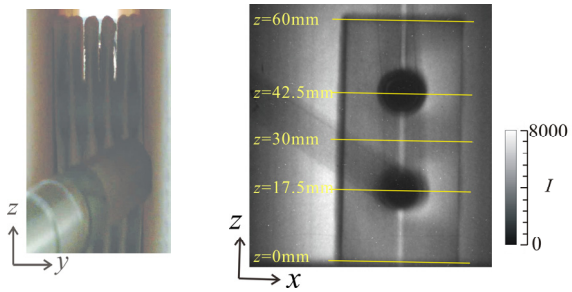

(a) Digital camera image (b) NRG image

Fig. 2 Digital camera image and NRG image

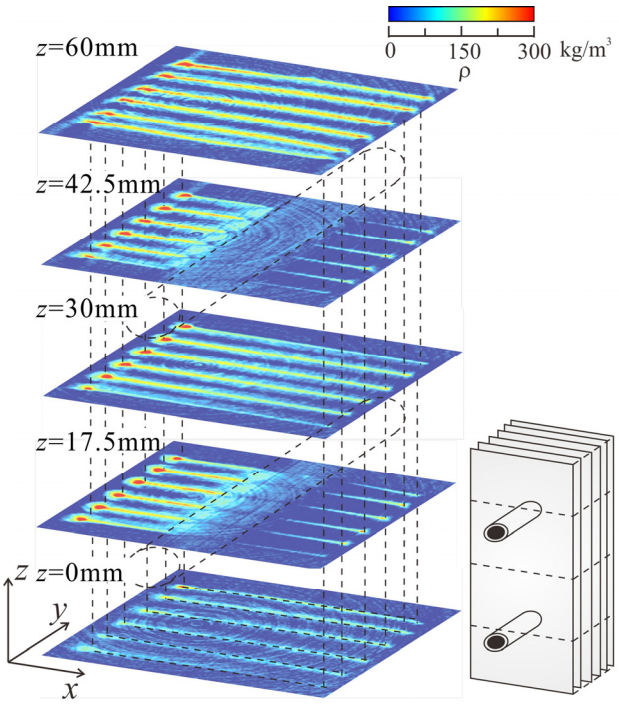

Fig.3 Three dimensional frost density distributions

REFERENCE:

[1] R. Matsumoto, et al., Proceedings of the International Heat Transfer Conference IHTC-15, IHTC15-9144, Kyoto, pp. 3603-3615

PR7-6 Study on the Visualization of Organic Matter between Metals in oder to Contribute to the Advancement of the Industrial Products

K. Hirota, H. M. Shimizu, M. Kitaguchi, Y. Tsuchikawa, S. Imajo, S. Awano, A. Uritani[1], K. Watanabe[1], S. Yoshihashi[1], A. Yamazaki[1] and Y. Saitoh[2]

Graduate School of Science, Nagoya University
[1]Graduate School of Engineering, Nagoya University
[2]Institute for Integrated Radiation and Nuclear Science, Kyoto University

INTRODUCTION: Mechanical and industrial products such as automobiles and aircraft are progressing with higher performance and higher accuracy in Japan. One of the demands at the development site of these state-of-the-art products is visualization of the state of organic films (oil film, grease, electrolyte, etc.) existing between metals, which can not be seen directly by our eyes. In this research, we will explore the possibility of observing the dynamic state of the organic film (shape, properties, thickness distribution) and its dynamic change mainly between automobile parts as an example.

At present Nagoya University is constructing an accelerator driven small neutron source (NUANS) and neutron radiography ports [1,2]. We are also proceeding with the quantitative evaluation of the difference in performance among the radiography ports by measuring and comparing the same sample with two devices. This year, we produced a camera for radiography to be used at NUANS, so we evaluated its performance in KUR E2 port.

EXPERIMENTS: The detector indicator was set at the front of the radiography camera box and evaluates the spatial resolution. Two camera boxes of used E2 and NUANS were measured for comparison. These two camera boxes were used same CCD and optics systems, almost same performance can be expected. The scintillator thickness dependence was also checked.

RESULTS: As shown in Fig. 1, clear radiography images are available to get by both camera boxes. The X-axis projections of the comb shape indicators are shown in fig.2, which left and right are reversed. We can see the almost 0.1mm resolution at all scintillator conditions. It is confirmed that the both camera boxes have almost same performance despite the increase of the white spots due to the radiation damage of long-term use at E2 port.

The ^{6}LiF/ZnS(Ag) scintillator thickness is also checked. The spatial resolution slightly drops at 200 microns thickness. This is because of the scintillating light spreading in the scintillator. The S/N ratio of the image for 200 microns thickness is better than for 100 microns.

These imaging camera box are useful for visualization of organic matter.

New imaging detector was also evaluated, which was LiF coated Si-pixel detector. Since this detector counts events where the output voltage above the threshold energy, gamma rays can be separated to some extent. Although CCD can not eliminate the contribution of gamma rays because it integrates charge, this detector can be excluded, so it is promising as a future neutron detector.

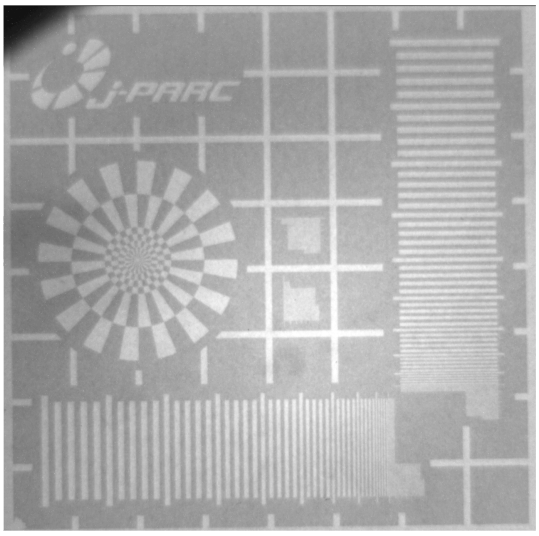

Fig. 1. The X axis projection image of the detector indicator.

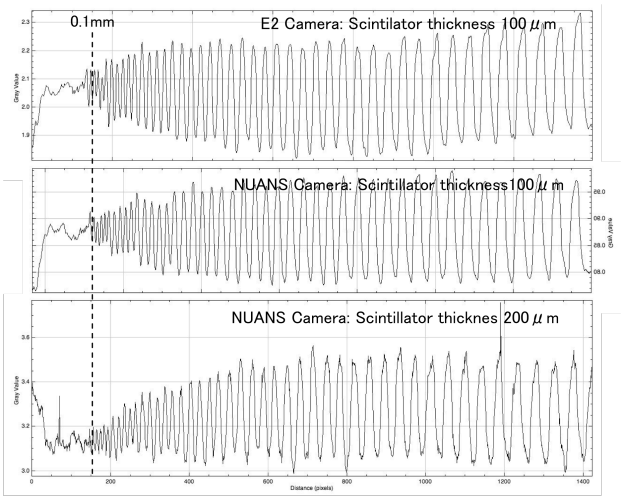

Fig. 2. The X axis projection image of the detector indicator.

REFERENCES:

[1] K.Hirota, PoS(KMI2017) 025.
[2] I.Ito, PoS(KMI2017) 068.
[3] X.Llopart, et.al., Nucl. Instrm. Meth. A**581** (2007) 485.

PR7-7

On the Luminescence of Helium Excimer Clusters Via Neutoron-3He Absorption Reaction

Y. Tsuji[1], T. Matsushita[2], V. Sonnenschein[1], K.Hirota[2], S. Suzuki[1], S. Kokuryu[1], D. Ito[3] and K. Saito[3]

[1]*Graduate School of Engineering, Nagoya University*
Department of Energy Engineering and Science
[2]*Graduate School of Science, Nagoya University*
Department of Physics
[3]*Graduate School of Science, Kyoto University*
Research Reactor Institute, Kyoto University

INTRODUCTION: Below about 2.17 K, liquid ^{4}He transits to the superfluid phase in which an inviscid irrotational superfluid component coexists with a viscous normal-fluid component. As a quantum fluid, superfluid helium exhibits many interesting properties. In recent ten years, new techniques have been applied to visualize the flow of superfluid helium and measure the local velocity fluctuation. Among these the most powerful one is the particle image velocimetry (PIV) which is a potential tool to measure the local velocity and promises to provide us a deep understanding of complex superfluid motions.

Helium excimers have advantages as a tracer particle of PIV such as, (i) the molecule size is several angstroms, (ii) a neutral particle in superfluid, and (iii) do not aggregate. The neutron-^{3}He absorption reactions proposed here is a possible method to generate small clusters of the helium excimers, which can be detected as individual tracer particles that follow faithfully the motion of the normal-fluid component in superfluid helium. This technique will allow unambiguous determination of the complete normal-fluid velocity field.

EXPERIMENTS: To observe the triplet He_2* excimers, the laser-induced fluorescence can be used. Figure 1 shows energy levels of a triplet excimer in liquid He. When 905 nm laser is applied, a 905 nm photon excites an excimer from the ground state *a* to the metastable state *c*, and then, it is further raised to the excited state *d* by absorption of another 905 nm photon. The *d* state decays to the *b* state, emitting a detectable 640 nm photon. Therefore, to excite the fluorescence, an excimer in the intermediate state *c* excited by one 905 nm photon has to meet another 905 nm photon within the *c* state lifetime approximately 4 nsec. When the *b* state relaxes back to the ground state *a*, the transition becomes cyclic and can be repeated during the lifetime ~ 13 sec of the triplet excimer. The sample liquid ^{4}He is stored in a stainless Dewar with 4 quartz optical windows. Space for liquid ^{4}He is 16 cm in diameter and about 1 m height. Neutron beam (B-4 line) with the cross section about 1 cm^2 is injected to the sample space through 2 quartz windows of Dewar.

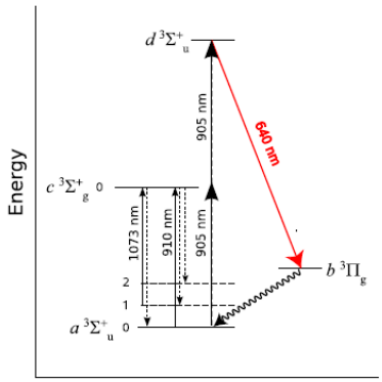

Fig. 1: Energy levels of a triplet He_2* excimer in liquid helium. *W.G. Rellergert et al., PRL **100**, 025301 (2008)*

RESULTS: Fluorescence from 640 nm photons are collected by detectors with 640 nm bandpass filters through the other 2 windows in directions perpendicular to the neutron beam, to avoid direct detection of laser photons. First, 2 photomultipliers are employed for the detector, and resulted signals are recorded for each 905 nm pulse. At this condition, the configuration of the excitation laser system is optimized, while the possibility of dark current is excluded. Figure 2 shows the results of signal recorded by photomultipliers. The sharp spike at 100 ns is the pump laser at 905nm pulse. Figure 2(a) and (b) are with neutron and without neutron, respectively. It is difficult to remove the background light completely, then they are recorded in Fig.2(a). It is clearly observed that the emission by helium excimer clusters via neutoron-3He absorption reaction in Fig.2(b).

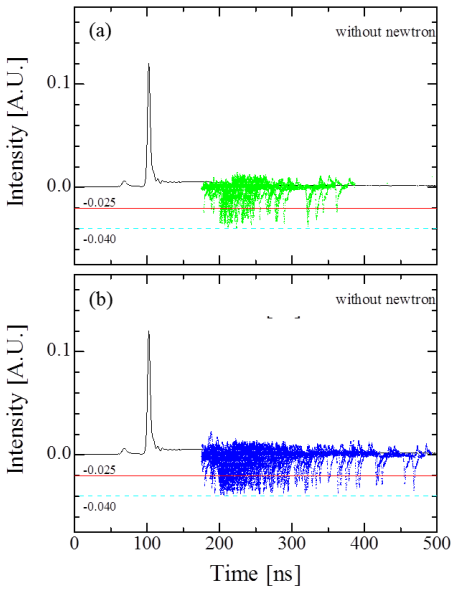

Fig.2: Recorded signal of photomultipliers.
(a)without neutron, (b)with neutron

PR7-8 # Development of Capillary-Plate-Based Flourescent Plates

T. Sakai, H. Iikura, M. Matsubayashi, D. Ito[1] and Y. Saito[1]

Materials Sciences Research Center, Japan Atomic Energy Agency

[1]*Research Reactor Institute, Kyoto University*

INTRODUCTION: Fluorescent plates are widely used for neutron radiography. In the case of the imaging devices, the spatial resolution of fluorescent plates conflicts with their detection efficiency. In general, a thicker phosphor layer increases the efficiency, but adversely affects the resolution because of blurring [1]. In this work, we developed a new approach to fabricate micro-structured fluorescent plates. The devices consist of capillary plates and fine phosphor grains [2]. Capillary plates are glass plates on which tiny capillaries are arrayed in two-dimensions periodically [3]. Herein, we introduce the development of fine fluorescent plates for neutron radiography imaging device.

EXPERIMENTS: The original capillary and phosphor-packed plates were observed using an optical microscope. The micrographs of the plates are shown in Fig. 1. All holes are clearly observed to be filled with the phosphor grains. The plate material was borosilicate glass. The specifications of the plates are as follows: plate thickness, 0.4 mm; diameter of each capillary, 25 μm; pitch of each hole, 31 μm; open area ratio, 59 %; diameter of effective area, 20 mm. The phosphor grains were sifted silver-activated zinc sulfide (ZnS:Ag) with a mean particle size of approximately 7 μm [1]. ZnS:Ag is one of the most popular phosphors because it exhibits excellent efficiency with a maximum emission wavelength of 450 nm [4]. The plates are impregnated with ^{10}B-enriched orthoboric acid to add neutron detection sensitivity.

The neutron imaging experiments were performed at KUR E-2. The images were collected using a CCD camera as shown in Fig. 2.

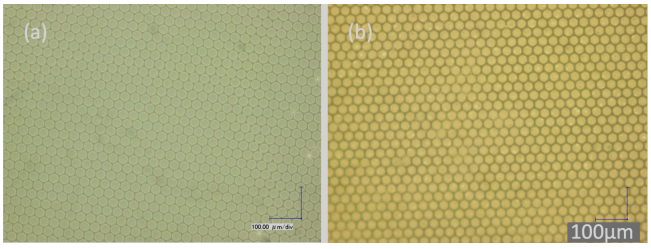

Fig. 1 Micrographs of the original (a) and phosphor-packed (b) capillary plates.

RESULTS: Neutron induced fluorescence is clearly observed and the fluorescence is relatively uniform. The spatial resolution is not evaluated yet, but the line-pairs are evident as shown in Fig. 2 (b).

We have developed the micro-structured fluorescent plates successfully. Microscopic images revealed that each capillary was well filled with phosphor grains and functioned as a microcolumnar fluorescent material.

Impregnation with ^{10}B-enriched orthoboric acid is effective to add neutron sensitivity to the fluorescent plates. The fabricated fluorescent plates are expected to be useful in high-spatial-resolution imaging devices with good detection efficiency. The next step of the work is to increase the neutron detection efficiency. The metal coating inside the capillary walls is considered to be a promising method.

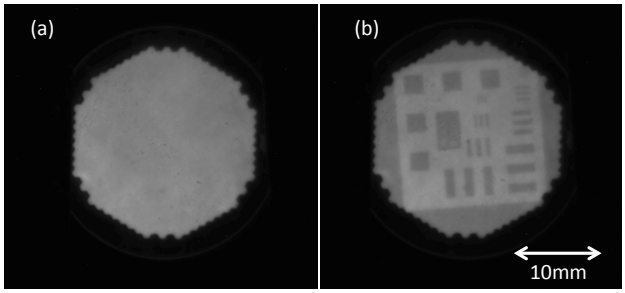

Fig. 2 Results of fluorescent plates neutron imaging. The plate was exposed to neutrons for 10 minutes. Images (a) and (b) are no object and a line-pair indicator [5] images, respectively.

REFERENCES:

[1] T. Sakai *et al.,* Nucl. Instr. and Meth. Phys. Res. B 332 (2014) 1238.

[2] T. Sakai *et al.,* JPS Conf. Proc. 11, 020005 (2016) .

[3] HAMAMATSU PHOTONICS K. K. website: <http://www.hamamatsu.com/jp/en/product/category/3200/3032/index.html>.

[4] Seung Kyu Lee *et al.,* Prog. in Nucl. Sci and Tech., Vol.1, (2011) pp.194-197.

[5] R. Yasuda *et al.*, Physics Procedia 43 (2013) pp.196-20.